The ROYAL COLLEGE *of* OPHTHALMOLOGISTS

REVIEW ARTICLE

Check for updates

Imaging of iris vasculature: current limitations and future perspective

Claudio Iovino [1], Enrico Peiretti[2], Mirco Braghiroli[2], Filippo Tatti[2], Abhilasha Aloney[3], Michele Lanza [1] and Jay Chhablani [4]✉

Fluorescein and indocyanine green angiography have been the traditional ways to image the vasculature of the iris in the last few decades. Because of the invasive nature of these procedures, they are performed in rare situations, and thus, our understanding about iris vasculature is very limited. Optical coherence tomography angiography (OCTA) is a noninvasive imaging method that enables the detailed visualization of the retinal and choroidal vascular networks. More recently, it has been also used for the examination of the iris vasculature in healthy and disease eyes. However, there is a lack of uniformity in the image acquisition protocols and interpretations in both healthy and pathological conditions. Artifacts of iris OCTA include shadowing, motion, segmentations errors, mirror effects. OCTA devices have an eye-tracking system designed for the posterior segment and the applications of these systems on the anterior segment can determine motion lines, vessel duplication, and vessel discontinuity. OCTA of the iris should always be performed under ambient room lighting to create miosis and reduce iris vasculature changes during the examination. In the near future, eye-tracking systems specifically designed for the iris vessels could permit the follow-up function, and the development of new OCTA metrics could reveal interesting applications of this new imaging technique.

INTRODUCTION

The evolution of anterior segment (AS) imaging techniques has resulted in considerable advances in evaluating the vasculature of healthy and pathological iris as well as in identifying differentiating features between benign and malignant lesions [1]. In the last decades, different imaging modalities have been proposed to study iris vasculature, with several advantages and disadvantages. Fluorescein and indocyanine green angiography (FA and ICGA) have been considered so far, the traditional way to visualize blood flow in the iris [2, 3]. Despite providing detailed information of the iris vasculature, FA and ICGA have several limitations due to the need for an experienced angiographer and the risks related to the dye injection [2, 4]. Optical coherence tomography (OCT) provides non-contact, rapid in vivo imaging of ocular structures, and has become a key part of evaluating the AS of the eye. Furthermore, OCT image-processing software has now allowed for combination of multiple scans, 3-dimensional reconstruction, and accurate measurements [5].

OCT angiography (OCTA) is a noninvasive emerging imaging technique that allows for simultaneous in vivo imaging of the vasculature in the eye without using any intravenous dye [6]. To date, most OCTA technology and algorithms have been optimized for the posterior segment. Further developments in AS OCTA have now allowed for evaluation of AS pathology such as glaucoma, ocular surface diseases, corneal vascularization, and abnormal iris vasculature [7–9]. Several authors investigated the feasibility of the OCTA in iris imaging in healthy eyes and in pathological

conditions, such as iris vessels malformations or tumors and iris neovascularization [10–12]. However, there are many sources of artifacts regarding iris OCTA (iOCTA) including projection, motion or blinking, masking, and segmentations artifacts [8, 13]. Moreover, there is a lack of uniformity in the image acquisition protocols and interpretations of both normal and disease eyes.

This review aimed to summarize the iris structural characteristics and analyze the technical aspects and applications of the available iris imaging modalities, focusing on iOCTA, its current limitations, and future directions.

METHODOLOGY

We conducted a comprehensive literature review using PubMed. The search terms used were "anterior segment ocular imaging", "iris vasculature", "iris vessels", "iris imaging", "iris fluorescein angiography"', "iris indocyanine green angiography", "iris optical coherence tomography", "iris optical coherence tomography angiography". A thorough search of peer-reviewed articles was conducted between 1 October 2020 and 1 March 2021. A few articles published before 1990 are included for historical purposes and the lack of research studies on the topic, but the review is based mainly on articles published in the past fifteen years. All searches were limited to the English language. Specifically, we were interested in the imaging techniques of the iris vasculature. This review included prospective and retrospective studies/series and other reviews. We included case

[1]Eye Clinic, Multidisciplinary Department of Medical, Surgical and Dental Sciences, University of Campania Luigi Vanvitelli, Naples, Italy. [2]Department of Surgical Sciences, Eye Clinic, University of Cagliari, Cagliari, Italy. [3]PBMA'S H. V. Desai Eye Hospital, Hadasapar, Pune, India. [4]UPMC Eye Center, University of Pittsburgh, Pittsburgh, PA, USA. ✉email: jay. chhablani@gmail.com
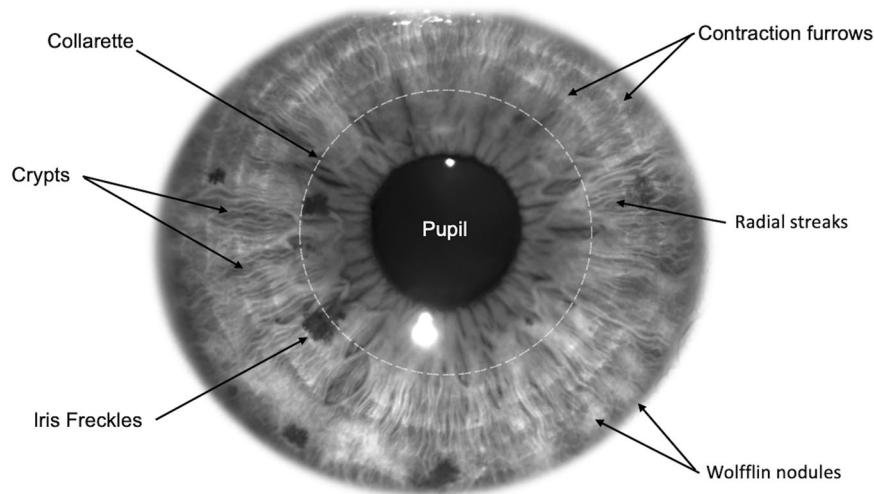
Fig. 1 Anterior segment color picture showing iris features. Dashed line demarcates the collarette region. Crypts are also visible among the radial streaks. Some iris freckles and Wolfflin nodules are dysplayed. The peripheral circular lines correspond to the contraction furrows.

reports only if they contributed new information about imaging of the iris vasculature.

ANATOMY OF THE IRIS
The knowledge of iris anatomy including its vasculature is a prerequisite for an accurate interpretation of iris images. The average diameter of the iris is 12 mm, and its thickness varies from the collarette to the root, respectively the thickest and the thinnest area [14].

Anterior surface of the iris
Iris is divided into two major regions. The pupillary zone is the inner region that forms the pupil boundary. The ciliary zone is the rest of the iris that extends to its origin at the ciliary body [14, 15]. The collarette is the thickest region of the iris, which lies about 2 mm from the pupil margin. The root of the iris is the thinnest and most peripheral part of the iris.

The anatomical variations in the anterior surface of the iris are unique in each individual. Representative image of the iris features is shown in Fig. 1. The iris is characterized by [14, 15]:

- Radial streaks composed of the underlying radial vessels.
- Crypts, defined as depressions where the superficial layer of the iris is absent.
- Contraction furrows, faint lines concentric to the collarette.

- Wolfflin nodules, white or orange nodules prominent in light iris color people.
- Brushfield spots seen in Down Syndrome people are similar to Wolfflin. nodules [16].
- Iris Freckles are pigmented spots that can change in size due to sun exposure [14, 15].

Posterior surface of the iris
The posterior surface of the iris is characterized by [14]:

- Schwalbe's radial contraction folds, a series of fine radial folds in the pupillary portion of the iris extending from the pupillary margin to the collarette.
- Schwalbe's structural folds, radial folds extending from the border of the ciliary and the pupillary zone that are much broader and more widely spaced.

- Some of the circular contraction folds, a fine series of ridges that run near the pupillary margin and vary in thickness of the iris pigment epithelium; others are in ciliary portion of iris.

IRIS HISTOLOGY
A brief histological description is also essential for a better understanding of the applications of iris imaging techniques. Cellular distribution and composition are variable in relation to the iris color [17]. Iris is the anterior part of the uvea and its root arises from the ciliary body [18]. It is constituted in an anteroposterior direction by anterior surface, stroma, sphincter and dilator muscles, and double layers of iris pigment epithelium [15].

The anterior surface of the iris is composed of fibroblast, collagen, and melanocytes and it is more pigmented in darker eye colors [17, 18]. Melanocytes can be spread or organized in nevi and freckles, showing variable pigment in different color eyes [17]. The stroma originates from the mesoderm and is composed of connective tissue, muscle fibres, blood vessels, nerves, and some melanocytes [17, 19]. Blood vessels are placed at different depths forming most of the volume of the iris and are radially oriented with multiple anastomosis [17].

The nervous system is represented by autonomic, sensory, vasomotor, and motor nerves. Other cellular components in the stroma are macrophages that contain pigment, multinucleated pigment cells, mast cells, lymphocytes, and plasma cells [17].

The sphincter and dilator muscles have a neuroectodermal origin. The dilator muscle has smooth fibers disposed in a radiating manner from the pupillary margin to the base of the iris. The contraction of this muscle increases the pupillary diameter. The sphincter muscle is a 1 mm wide band disposed concentrically at the margin of the iris, circling the pupil. It is continuous with the anterior layer of the iris by a thin layer of connective tissue. The sphincter muscle contraction causes the constriction of the pupil [17, 19].

The most posterior surface of the iris corresponds to the iris pigment epithelium. It originates by the invagination of the embryonic optic cup on itself and it is formed by two layers of pigmented cells. These two layers can be divided into anterior and posterior iris pigment epithelium layers. The cells of the anterior layer have tight junction desmosomes, however, there are some areas of separation between them. In these areas, there are microvilli with rarely cilium. The posterior layer contains a lot of melanin pigment granules and shows tight junctions and

desmosomes on the lateral and apical walls [17]. Overall, the color of the iris depends on the amount of pigment in the stroma, because the pigment in the posterior epithelial layers is relatively constant between individuals [18].

IRIS VASCULATURE

Normal iris vessels are located in the iris stroma, covered by anterior surface layer, and may not be visible in slit lamp examination in darkly pigmented eyes [20]. The iris is mainly supplied by anterior ciliary arteries (ACA), the long posterior ciliary arteries (LPCA), and anastomotic connections from the anterior choroid [21]. The ACA and LPCA anastomose at the level of the ciliary body and form two successive arterial circles:

- The minor arterial circle located in the stroma of the iris
- The major arterial circle found in the stroma of the ciliary body

The minor arterial circle is found along the border of the pupil and is linked by radially oriented vessels within the iris stroma [21].

The veins follow the arteries and converge to a minor venous circle in the iris. This circle empties into the vorticose veins, that belong to the system of ophthalmic veins.

In an interesting study by Song et al. normal iris vascular network was studied using a flat preparation using fluorescent and light microscopies [22]. LPCA formed several branches before entering the iris root, and such branches formed the major arterial circle of the iris with diverse diameters in the vicinity of the iris root and the ciliary process [22]. In the pupillary margin, the iris vasculature network formed a cone shape and then formed an arcade by connecting to adjacent vasculatures. In the vicinity of the collarette, the iris vasculature network formed the minor arterial circle of the iris with diverse diameters perpendicular to the arcade of the iris network located in the pupillary margin. In the pupillary margin, the capillaries were somewhat thick and connected to the irregular traveling iris veins [22]. However, a limitation of this study was that the ciliary body and the iris were separated during the preparation of the iris, hence the contribution of the ACA to the formation of the major arterial circle of iris could not be assessed [22].

The ACA flows mostly to the anterior uvea. It travels in parallel to the rectus muscles, penetrates the sclera, and forms intramuscular loops by generating many branches in the external layer of the ciliary muscles. It also forms the major arterial circle of the iris together with the LPCA, which is the major blood supplier to the iris and the ciliary body [23]. Interestingly, Hayreh et al. have reported that the temporal branches of the ACA and LPCA have less influence on the blood supply to the temporal portion of the iris than do the nasal, superior, and inferior portions, based on FA taken after strabismus surgery [2].
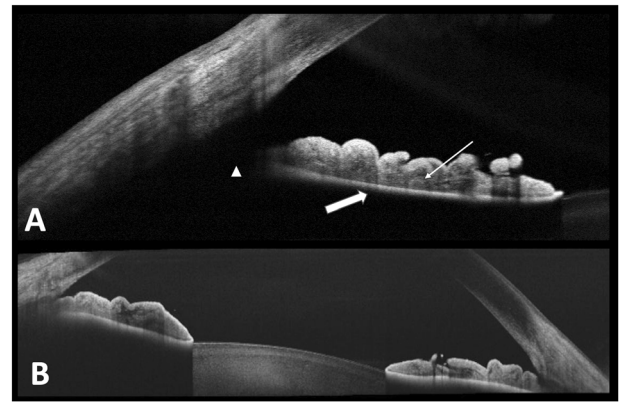
ANTERIOR SEGMENT OPTICAL COHERENCE TOMOGRAPHY OF THE IRIS

OCT was initially developed to provide detailed cross-sectional images of the posterior segment such as the retina and the optic nerve head [24]. However, it was not until 1994 that Izat et al. reported the first AS-OCT evaluation [25]. The AS-OCT provides visualization and analytics of clinically relevant AS structures, including the iris.

Anterior segment optical coherence tomography of healthy iris

On AS-OCT only 2 iris tissue subdivisions can be made: the anterior border/stromal layer and the iris pigment epithelium [26], as shown in Fig. 2A.

Although several methods of measurement have been described, OCT provided a reliable imaging technique for iris

Fig. 2 **Spectral-domain (SD) and swept-source (SS) optical coherence tomography (OCT) of the iris. A** SD-OCT of the iris in a 30 years-old man acquired with Optovue Angiovue, showing the anterior border/stromal layer (thin arrow) and the iris pigment epithelium (thick arrow). Arrowhead shows the failure to identify the anterior iris surface beneath the Schwalbe's line. **B** Swept source-optical coherence tomography of the iris in a 36 years-old woman acquired with Topcon Triton showing an excellent visualization of the peripheral iris.

thickness evaluation both in pathological conditions and in healthy subjects [27, 28]. Invernizzi et al. reported that iris thickness varies by sector, iris color, age, and sex in healthy eyes as evaluated on AS-OCT [29].

A previous study, analyzing iris surface features and their relationship with iris thickness measured by AS-OCT, reported that irides with more crypts were thinner, while irides with more furrows were associated with thicker peripheral iris. Furthermore, the authors found that darker irides were thicker, probably due to the higher melanocytes and melanin content in the stroma [30].

Interestingly, AS-OCT allows also the analysis of the geometry of the iris. Shuster et al. reported an association between the existence of a concave iris configuration and myopia, younger age and male gender, whereas, in the same study, a convex iris configuration was associated with hyperopia, older age, and female gender [31].

Despite the advantages of AS-OCT, several imaging technique errors and artifacts have been described [32]. According to preceding studies conducted focusing on the measurement of the anterior chamber angle, the AS-OCT images needs to meet the requirement of some elements, such as the light-controlled pupil dilatation and a clear iris surface beneath Schwalbe's line [32]. Furthermore, the distance between the light source and the tested eye could influence the accommodation state, which could affect the pupil size and subsequently the iris evaluation [33].

The adoption of specific measure should be necessary for the OCT evaluation of the iris. The failure to identify the anterior iris surface results in the inability to evaluate the angle opening distance under Schwalbe's line and to measure the exact peripheral iris thickness [32].

AS swept source (SS)-OCT, with a faster scanning speed and longer wavelength allows for high-resolution, deep-penetration images of the entire anterior segment, including the iris (Fig. 2B) [33].

Anterior segment optical coherence tomography of the iris in anterior uveitis

Changes in the iris thickness are often reported as a typical sign of anterior uveitis [29]. AS-OCT allows the visualization of various features of the AS, including not only the iris thickness but also anterior chamber depth, presence and extent of anterior synechiae, iris bowing, and angle lesions. It could thereby be
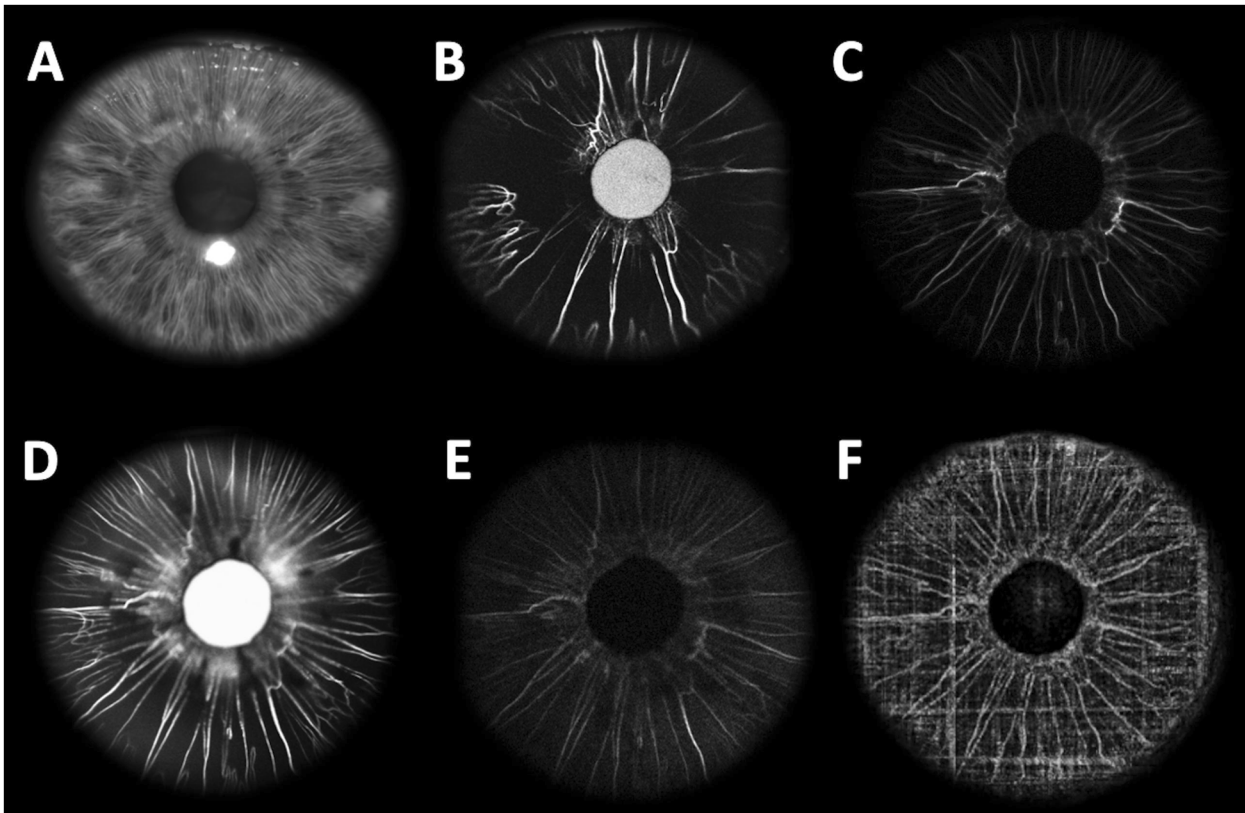
Fig. 3 Multimodal imaging of a light-colored iris of a 52-years-old healthy patient with the normal undilated pupil. A Anterior segment colour picture shows a light blue-green iris. **B, C** Early phase fluorescein and indocyanine green angiography (FA and ICGA) of the iris display the arterial vascular filling starting from the root of the iris with a radial orientation. **D, E** Late phase FA and ICGA show a dense plexus of capillaries in the pupillary region. Note a late leakage of the dye on late phase FA (**D**). **F** Optical coherence tomography angiography performed before dye injection clearly shows the minor arterial circle found along the border of the pupil linked with the radially oriented vessels.

used for the diagnosis and management of anterior uveitis [34]. A diffused iris thinning on OCT has been described in Fuchs uveitis, as well [35].

Anterior segment optical coherence tomography of the iris in glaucoma

Several reports analyzing iris features on AS-OCT have been published. Some authors reported that a decreased iris thickness and an increased iris convexity on OCT could contribute to angle closure [5, 36–39]. Furthermore, the AS-OCT could be used as a helpful tool in the management of angle-closure glaucoma, due to its capability to monitor changes to the anterior chamber angle after laser iridotomy [40].

Shah et al. reported the use of AS-OCT to delineate the iris profile in patients affected by pigment dispersion syndrome [41].

Anterior segment optical coherence tomography in iris tumors

It has been well established that AS-OCT could be a reliable alternative in following some selected nonpigmented iris tumors [42–44]. Nevertheless, due to its penetration deficit, AS-OCT suffers from optically-related image shadowing with large, pigmented, iris pigment epithelium and ciliary body lesions [45, 46].

Ultrabiomicroscopy and ultrasound B-scan showed their superiority to AS-OCT in imaging of larger iris lesions [43–46], although AS-OCT could be a useful noninvasive tool for evaluation and management of small nonpigmented anterior iris tumors [43–46].

CONVENTIONAL IRIS ANGIOGRAPHY

First FA of the iris was described in 1968, however, the brown pigment masked fluorescein transmission [47]. ICGA has excellent pigment epithelium penetration compared to FA and therefore, has potential applications in detecting perfusion changes in dark irides [47]. Nevertheless, knowledge of iris angiography is limited and the procedure is not routinely performed. In this section, we will be focusing on the methods, advantages, and disadvantages of conventional FA and ICGA of the iris. Representative cases of FA and ICGA in light and dark iris are shown in Fig. 3 and Fig. 4.

Fluorescein iris angiography

Hayreh et al. in 1978 studied iris angiography pattern in 42 normal blue or green eyes to investigate normal vasculature pattern and in vivo circulation of the iris [2]. Brown eyes were unsuitable for angiography because brown pigment masked fluorescence. Iris FA was performed after intravenous injection of 5 ml of 10% or 2 ml of 25% sodium fluorescein solution. The study was performed in normal undilated pupils without the use of any prior medications. Unlike retinal FA, the iris FA revealed a much more complex pattern in the iris with interindividual variations in dye filling. These variations are considered physiological and may be misinterpreted as pathological.

Radial arteries of the iris filled rather sluggishly and the circulation in the pupillary and the peripupillary region was often much slower than in the peripheral part of the iris. The filling of iris segments was variable, but it was observed that the nasal part was the first to fill and the temporal part last. It was seen that the
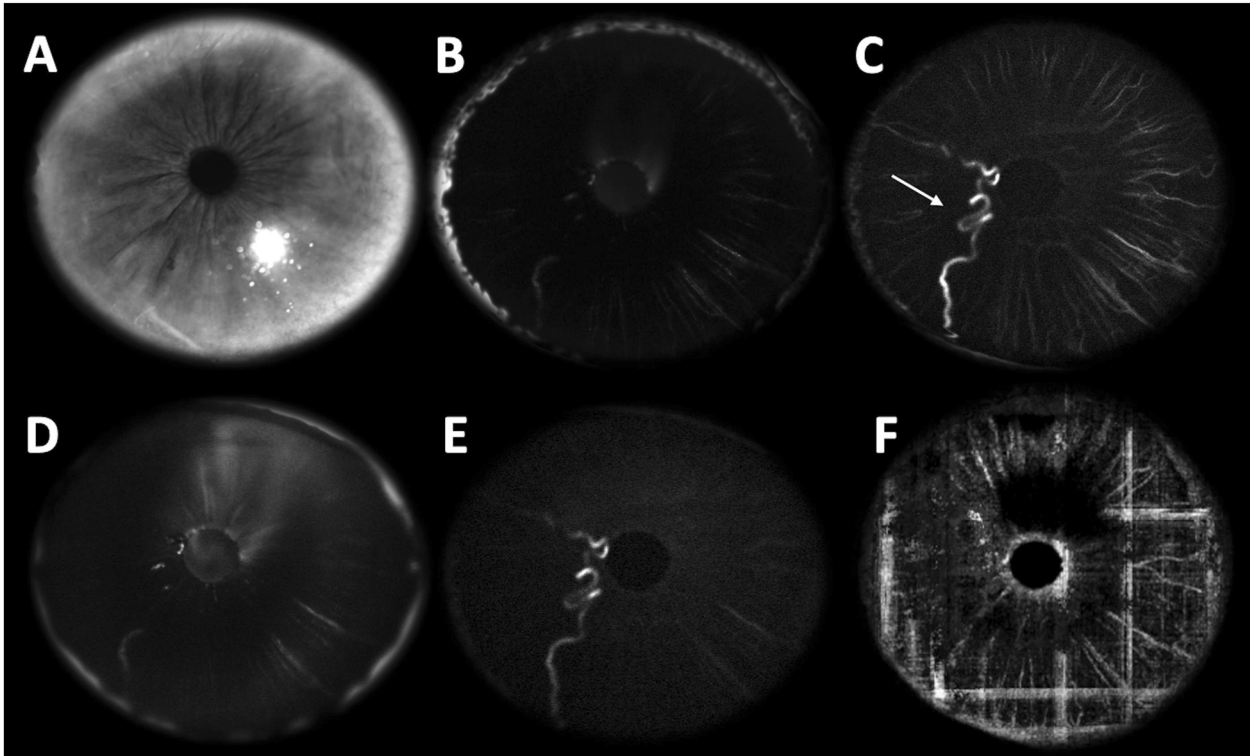
Fig. 4 Multimodal imaging of a pigmented iris of a 57-years-old healthy patient with normal undilated pupil. A Anterior segment colour picture shows a brown iris and corneal gerontoxon. **B** Early phase fluorescein angiography (FA) of the iris shows how the pigment impairs the evaluation of the vasculature. **C** Early phase indocyanine green angiography (ICGA) allow the imaging of some vessels, including a vessel with anomalous orientation (white arrow). **D**, **E** Late phase FA and ICGA still show a difficult evaluation of the iris vasculature. Note a late leakage of the dye in the superior pupillary margin on late phase FA. (**F**) Optical coherence tomography angiography performed before dye injection shows flow artifacts and multiple masking effects making the quality of the image very low.

blood flow in the iris is usually much slower than in the choroid or the retina. The arterial channels could easily be recognized because they filled first of all from the root of the iris and from their mostly radial orientation. There was no distinct venous phase, but it merged with the arteriovenous phase. It was also observed that the pupillary region of the iris between the collarette and the pupillary margin contained a dense plexus of capillaries [2].

In another study by Gillies and Tangas on iris angiography in eyes with pigment dispersion syndrome, the arterioles and venules were seen to run in a radial pattern, but the veins were more numerous and deeper compared to arterioles [48]. The arterioles filled 9–20 or more seconds after the dye was injected in the arm and the veins filled four seconds after the arterioles [48].

Indocyanine green iris angiography
Indocyanine green (ICG) has a peak absorption at 790–805 nm and it fluoresces at 825–835 nm [49]. Only 10% of the light is absorbed at this infrared range, hence the dye can be seen through overlying haemorrhage, melanin, fluid, xanthophyll, etc. Due to the ability of this dye to fluoresce at a wavelength not blocked by overlying pigment, the ICGA of the iris become a potential diagnostic tool even in brown irides [47]. Chan et al. showed how the filling of the dye started at variable locations peripherally from the iris root, the nasal area tended to fill first and the temporal area followed [47]. The superior and inferior portions filled in intermediate phase between the nasal and temporal filling.

The radial arterial vessels joined in an incomplete circumferential pattern around the collarette, forming the minor arterial circle of the iris. Filling of the whole iris usually required

5–10 seconds [47]. The advantage of ICGA over FA is mainly that the iris colour does not affect the imaging capability of the ICGA. It has further advantage of being a protein-bound molecule intravascularly which allows for very precise evaluation of iris hypoperfusion [47].

Disadvantages of conventional iris angiography

- Invasive procedure
- Requires skilled technician: in slightly out of focus angiograms, the iris vessels appear blurred giving an erroneous impression of leakage [2]. This artifact may be misinterpreted by clinicians.
- Time-consuming: of the three visible ocular circulatory systems- choroid, retina, and the iris- the iris is the slowest [2]. Therefore, iris angiography takes more time compared to retinal angiography.
- Limited application in people with systemic comorbidities, liver and kidney diseases, patients allergic to dye, as well as pregnant women.

OPTICAL COHERENCE TOMOGRAPHY ANGIOGRAPHY OF THE IRIS
OCTA was introduced to study retinal and choroidal vascularization, without any dye injection [50]. Only in the last few years, OCTA has been applied to the AS of the eye [20]. Nevertheless, the majority of these reports are focused on corneal and conjunctival diseases. Recently, OCTA was demonstrated to be a reliable imaging technique to follow-up and monitor corneal vasculariza-

tion after anti-vascular endothelial grow factor treatment in the rabbit model [51, 52]. However, the current literature about the iOCTA is very limited[53]. This is mainly due to the technical limitations of the available machines. Several authors investigated the iris vasculature by means of OCTA in healthy eyes [7, 8]. Moreover, OCTA has been used to characterize iris ischemia after strabismus surgery [54], characterize the presence and response to treatment of iris neovascularization [7, 12, 20, 55, 56], analyze the vascularization within iris lesions/tumors [11, 57, 58], and in acute anterior uveitis [59]. It can also be useful for assessing the effects of anterior segment implants, such as iris-supported phakic intraocular lenses [8].

In this section, we summarize available devices, tips to obtain good iOCTA images, and challenges.

Available devices and algorithms

There are several commercially available OCTA devices, but only few of them have been used to investigate the iris vasculature [60–62].

The following different algorithms have been employed to produce iOCTA images (Table 1): split-spectrum amplitude-decorrelation (SSADA), complex difference, full-spectrum probabilistic approach, complex optical microangiography (OMAGc), OCTARA.

All the aforementioned OCTA systems are designed to mainly evaluate the posterior segment and there is a lack of scanning protocols specifically designed to assess the vascularity of the AS of the eye [6]. Nevertheless, with some tips and precautions the iris vasculature can be investigated as well.

For most OCTA machines, dedicated AS lenses are needed to image the iris due to focus mismatch issues. Ayres et al. created a dedicated lens built with a 3D printer and mounted on the 30° Heidelberg system [63]. This was done to use the retinal OCTA software for the iris vessels evaluation, since OCTA software got disabled by mounting the AS lens supplied by the manufacture. This is not true for all other devices for which the specific AS lens can be mounted and the retinal OCTA software can be used to image the iris vessels, as for the Optovue AngioVue® which allows to perform iOCTA with [7, 8, 12, 54, 64], or without the AS lens [10, 11, 58, 59, 65]. Whether the AS lens is mounted or not, it is also necessary to manually move the focus of the machine to the level of the tissue to be examined.

iOCTA must always be performed under ambient room lighting to create miosis and reduce iris vasculature changes during examination. The scan size, as for the OCTA of the retina, influence the final quality of the image. With a 6 × 6 scan you can get generally a whole caption of the iris, but the 3 × 3 cube scan allows for better vessels details.

Practical challenges and tips

There are several factors to consider when evaluating an iOCTA scan. It is important to understand how to recognize artifacts and avoid them in order not to make incorrect interpretations of OCTA images [13, 66]. Artifacts of iOCTA include shadowing, motion, segmentations errors, mirror effects, artifacts due to cornea opacities. As previously stated, OCTA devices have an eye-tracking system designed for the posterior segment [61].

The applications of these systems on the AS can lead to motion errors which determine motion lines, vessel duplication, and vessel discontinuity due to pupil changes and eye movement [61, 67]. Additionally, it is not possible to set reference in order to make follow-up comparative scans due to the great variability of the pupil size at each visit [53, 61]. A further important challenge is related to the iris color: darkly pigmented irides have shown reduced flow signal and more artifacts when compared to lighter coloured irides (Fig. 5) [60]. All these critical issues make the examination still difficult, with low reproducibility and repeatability.
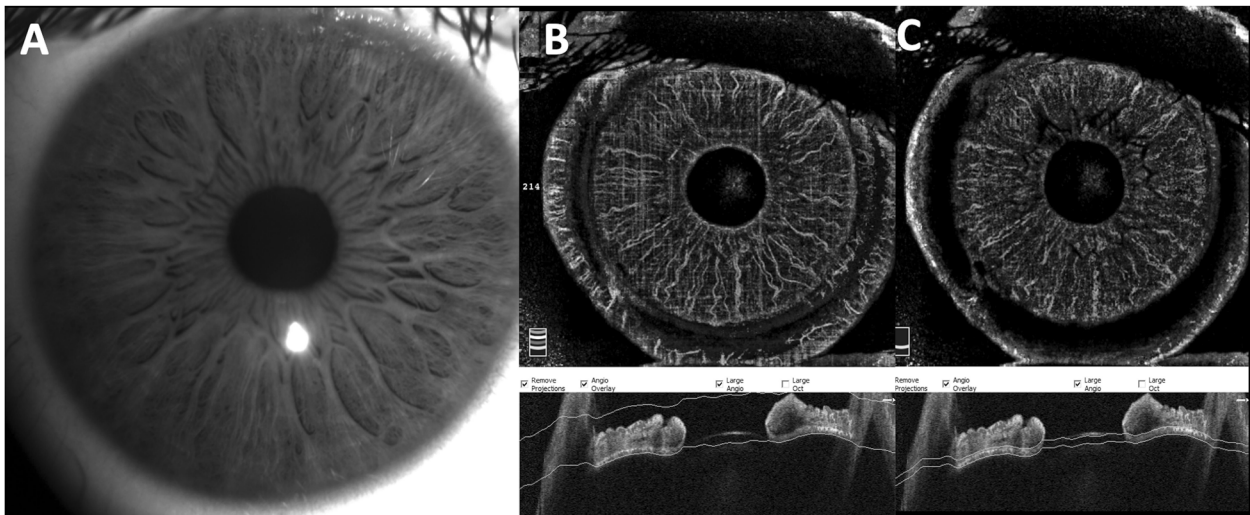
Table 1. Optical coherence tomography angiography devices used to investigate the iris vasculature.

OCTA device	RTVue XR AVANTi; SD-OCT	PLEX Elite 9000; SS-OCT	Spectralis OCT2; SD-OCT	RS-3000 Advance; SD-OCT	DRI Triton; SS-OCT
Manufactory	OptoVue, Fremont Inc., Calif., USA	Carl Zeiss Meditec Inc., Dublin, Calif., USA	Heidelberg Engineering, Heidelberg, Germany	Nidek, Aichi, Japan	Topcon Corporation, Tokyo, Japan
System	AngioVue™	AngioPlex™	Spectralis® OCTA	AngioScan™	SS OCT Angio™
Algorithm	SSADA	OMAGc	Full-spectrum probabilistic approach	Complex Difference	OCTARA
Scan speed (A-scan/s)	70000	100000	85000	53000	100000
Imaging depth (mm)	2.0–3.0	3	2	2.1	2.6
Macular scan area (HxV, mm2)	3 × 3, 6 × 6, 8 × 8	3 × 3, 6 × 6, 9 × 9, 12 × 12	3 × 3, 6 × 6	3 × 3 to 9 × 9	3 × 3, 4.5 × 4.5, 6 × 6, 9 × 9, 12 × 12
Scan range (HxV)	45 × 5	67 × 45	30 × 30	40 × 30	45 × 45
Eye-tracking technology	DualTrac™	FastTrac™	SMARTTrack™	Real-time SLO Eye HD Tracer	TruTrack™ Active Eye Tracking

HD High Definition, *iOCTA* Iris Optical Coherence Tomography Angiography, *OCTA* Optical Coherence Tomography Angiography, *OCTARA* Optical Coherence Tomography Angiography Ratio Analysis, *OMAGc* Optical Microangiography complex, *SD-OCT* Spectral Domain Optical Coherence Tomography, *SLO* Scanning Laser Ophthalmoscopy, *SSADA* Split-Spectrum Amplitude Decorrelation, *SS-OCT* Swept Source-Optical Coherence Tomography.
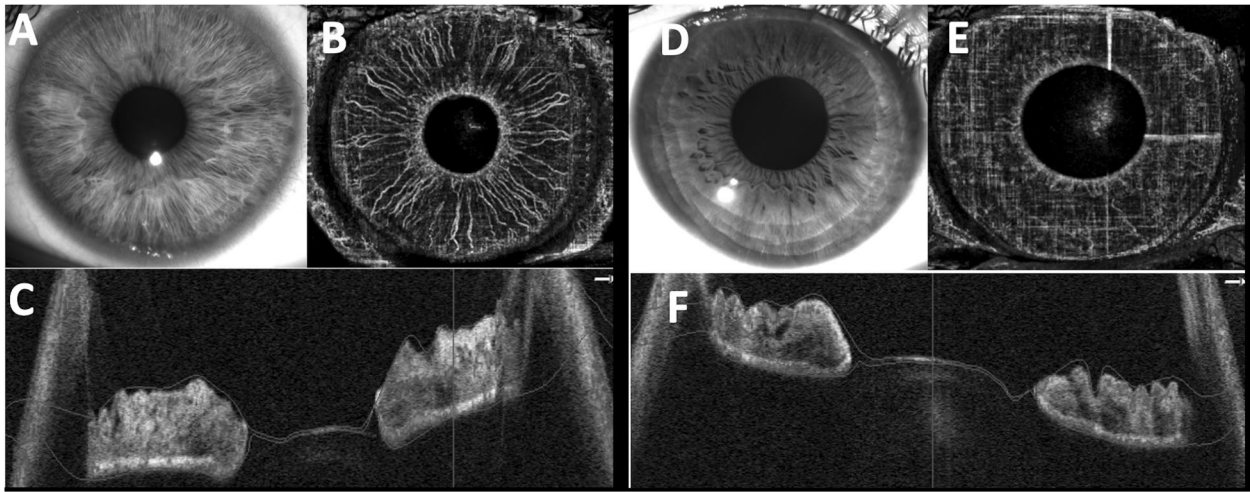
Fig. 5 **Spectral-domain optical coherence tomography angiography (SD-OCTA) of the iris of two young patients (30 and 32 years-old) with different pigmentation of the iris, acquired with Optovue Angiovue. A** Anterior segment slit lamp picture shows a light-coloured iris. **B** En face SD-OCTA of the iris allows a good visualization of the minor arterial circle along the border of the pupil linked with the radially oriented iris vessels within the stroma. Note the roundish peripheral shadowing effect at the iris root on en face scan due to the reflection of the cornea as shown on B-scan. **C** Manually adjusted B scan segmentation including all the iris tissue. **D** Anterior segment slit lamp picture reveals a brown dark iris. **E** En face SD-OCTA of the iris shows how the anterior pigment layer determines shadowing and flow artifacts that impair the iris vasculature evaluation. Note the roundish peripheral shadowing effect at the iris root on en face scan due to the reflection of the cornea as shown on B-scan. **F** Manually adjusted B scan segmentation including all the iris tissue.

Fig. 6 **Spectral-domain optical coherence tomography angiography of the iris of a 32 years-old man acquired with Optovue Angiovue. A** Anterior segment colour picture showing a brown-green iris. (**B**) Custom segmentation manually adjusted to include all the iris tissue showing a better visualization of the radially oriented iris vessels. Note the roundish peripheral shadowing effect at the iris root on en face scan due to the reflection of the cornea as shown on B-scan. **C** Custom segmentation manually adjusted to include only the pigment epithelium of the iris. Note the projection of the superficial iris vessels on en face scan with a more pronounced roundish shadowing effect and the red flow signal within the segmentation slab of the B scan.

Another source of biases is related to the shadowing effects. It is particularly important in eyes with corneal opacities or gerontoxon (Fig. 4) [8, 10, 61]. The reflection of the cornea on the iris causes a light scattering responsible for a roundish shadowing on the flow signal in correspondence of the iris root (Figs. 5 and 6). Automatic segmentation which is not designed for the iris structure represents one of the main issues of the iOCTA evaluation. Despite not being programmed for recognizing iris different vasculature layers, OCTA devices provide an automated segmentation, which most of the time requires manual adjustments to properly delineate iris boundaries [61]. Moreover, as for the OCTA of the retina, the iris pigment epithelium layer can cause

a reflection of the superficial layers (mirror effect) [68], and this is particularly evident with the choriocapillaris slab (Figs. 6 and 7).

Swept source-optical coherence tomography angiography of the iris
SS-OCTA systems with a longer wavelength (1050 nm) enable better penetration of the light source to deeper layers of the eye [68, 69].

Ang et al. compared SD-OCTA and SS-OCTA in delineating normal iris vessels and iris neovascularization in eyes with pigmented irides [7]. The two compared OCTA systems were the Angiovue SD-OCTA and the Plex Elite 9000 SS-OCTA. Both AS-
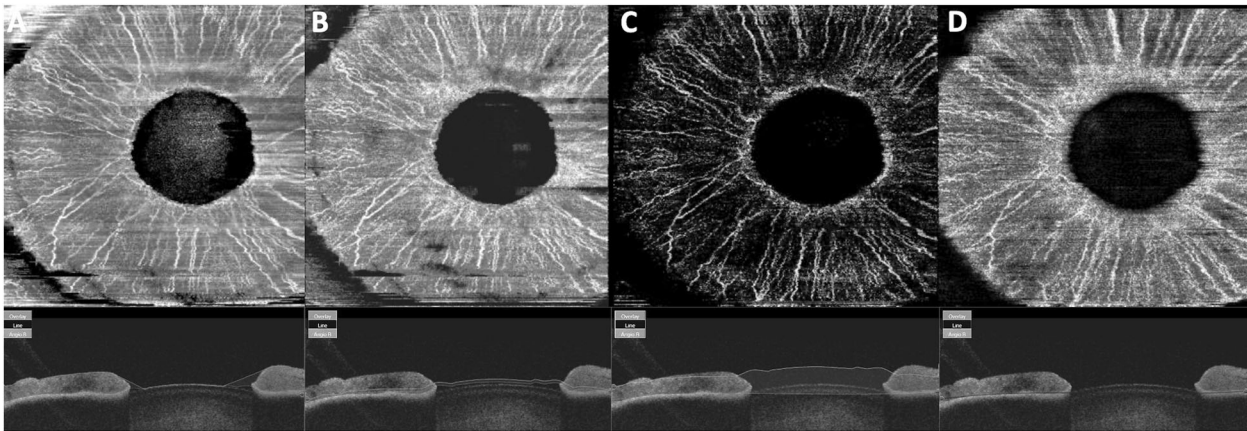
Fig. 7 Swept source-optical coherence tomography angiography of the iris of a 47 years-old woman acquired with Topcon Triton OCTA with the spacer and without the anterior segment dedicated lens. Macular 4.5 × 4.5 cube acquired moving the focus on the + level, showing en face and corresponding B-scans with automatic segmentations of superficial plexus (**A**), deep plexus (**B**), outer retina plexus (**C**), and choriocapillaris slab (**D**).

OCTA devices were able to detect iris neovascularization as they are usually more superficial on the anterior layers of the iris. Nevertheless, normal iris vessels, located in the iris stroma and not well visualized when blocked by dense iris pigments, were better delineated with SS-OCTA [7].

Triton DRI-OCT (Topcon Corporation, Tokyo, Japan) is a SS-OCTA that reaches up to 100,000 A-scans per second, and the algorithm in use is the OCTARA [5]. To focus on the AS the manufacture provides a specific lens and a head rest attachment [10]. There is only one paper in the literature reporting the SS-OCTA features of iris cysts imaged with Triton DRI-OCT [62]. Nevertheless, the authors did not give any detail of the methodology applied, and a 3 × 3 retinal cube was used to image only one sector of the iris [62].

We hereby propose some tips to circumvent challenges with Topcon SS-OCTA:

1. Acquisition protocol: The devise has not a dedicated software for the iOCTA and the macular protocol scan must be applied to the iris imaging. The follow-up function should be disabled. The 6 × 6 macular cube is the best scan size that allows to visualize all the iris without losing vascular details.

2. Use of specific AS lens: There are two options, the first of which is to mount the lens without making the final lock in order to deceive the machine sensor which does not recognize the attached lens. In this way it is possible to perform the iOCTA.

   The second option is to remove the AS lens and perform the iOCTA by moving the manual focus on the level + and then clicking the optimize signal button to improve the quality signal (Fig. 7). Nevertheless, in selected cases it can be difficult to start imaging capture because the software does not recognize the iris structure. For both options the head rest attachment is recommended.

3. Dilation: Mydriatic eye drops must be avoided because pupil dilation makes the image quality worse (Fig. 8).

4. Room light: An ambient room lighting is mandatory to create a discrete miosis and the same light setting should be used at each visit.

5. Segmentation tricks: As for all other manufactures, a manual adjustment of the automatic segmentations may be needed to trace the boundaries of the iris. Moreover, the choriocapillaris slab typically shows the mirror effect (Figs. 7 and 8).

FUTURE DIRECTIONS

Imaging of iris vasculature is evolving rapidly. Different scan patterns could allow for easier iOCTA imaging capture and dedicated software could facilitate the image analysis process. OCTA can produce high-resolution cross-sectional images, which can be segmented into different layers, allowing visualization of vessels at different depths. Artefacts due to non-parallel segmentation and the lack of a reliant eye tracker for iOCTA imaging can be avoided with developments in eye tracking and image registration specifically designed for iris vessels. Automated programs which already exist for AS OCT may be further developed to include iOCTA segmentation in the future. Some of the more interesting and recent innovations in medicine and ophthalmology come from the use of Artificial Intelligence (AI) [70–72]. AI enables to acquire information about a specific working situation and obtain strategies to improve the quality of that work [73]. In particular, it would be interesting to create some database of OCTA images of healthy and diseased irides. Using machine learning techniques, it would be possible to create some algorithms that help the ophthalmologist in detecting specific diseases or in differential diagnosis (i.e. benign vs malignant iris tumors).

CONCLUSIONS

Understanding about the iris vasculature and its clinical importance is increasing with advancing noninvasive imaging techniques. The current standard for characterizing anterior segment vasculature is iris angiography (FA and ICGA), despite substantial limitations as the need of dye injection [2, 4]. OCTA allows for rapid, noninvasive imaging of vasculature within the eye and it is better tolerated and more accessible than traditional angiography [67]. SS-OCT is characterized by high reproducibility of the measurements on the AS of the eye, as demonstrated in previous studies [69, 74]. The rapid scan acquisition and deeper tissue penetration did enhance many of our understandings [75]. Nevertheless, further studies are required to confirm the advantages, limitations, and differences between SS-OCTA and SD-OCTA, and between different OCTA systems for the AS vasculature analysis [76]. Moreover, commercially available systems are designed and optimised for the posterior segment vasculature analyses [6, 77, 78]. AS-OCTA is a new imaging field and many areas still require technical fine-tuning. New iOCTA software able to reduce projection and motion artifacts, allowing for a better-automated iris layers segmentation, are needed.
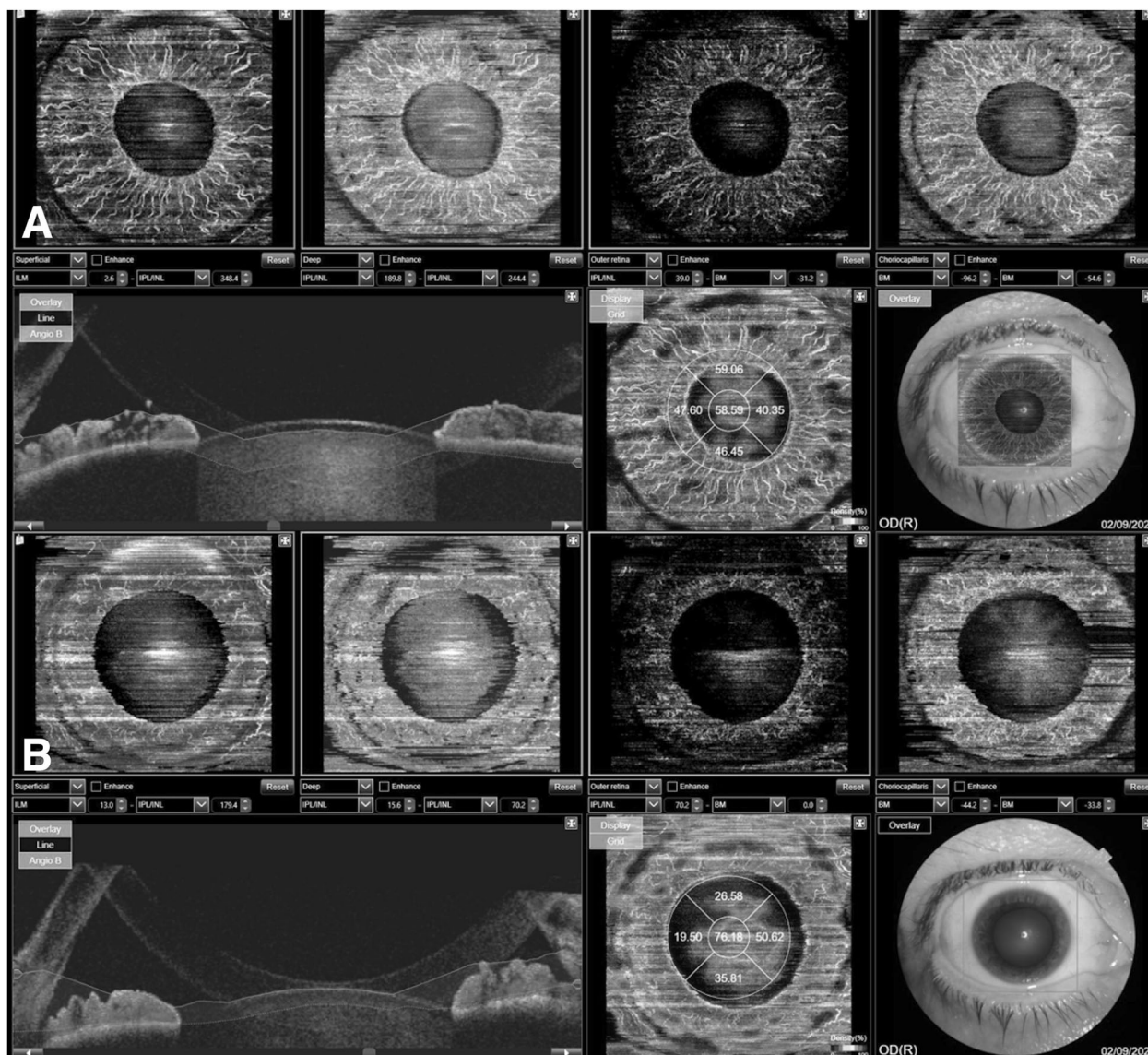
Fig. 8 Swept source-optical coherence tomography angiography of the iris in a 61 years-old man with brown iris acquired with Topcon Triton plus with spacer and without anterior segment lens before and after pupil dilation. Both scans were acquired with the same light room conditions. (**A**) 6 × 6 macular cube acquired before pupil dilation. (**B**) 6 × 6 macular cube acquired after pupil dilation. Note how the visualization of the iris vessels was worse after dilation.

OCTA finds fertile soil in inflammatory eye diseases as vascular changes in the iris, retinal, and choroid are the core sites of the pathophysiology of eye inflammation. Once algorithms and protocols have become well established, quantitative analysis of anterior segment pathologies could be performed and iOCTA may find many applications in AS disease diagnosis and management.

Therefore, many of the previously mentioned limitations may be addressed in the near future. Larger scale studies will be needed to validate the methodology and allow for standardization of iOCTA.

REFERENCES

1. Han SB, Mehta JS, Liu YC, Mohamed-Noriega K. Advances and clinical applications of anterior segment imaging techniques. J. Ophthalmol. 2016;2016:8529406.
2. Hayreh SS, Scott WE. Fluorescein iris angiography: I. Normal Pattern. Arch Ophthalmol 1978;96:1383–9.
3. Parodi MB, Bondel E, Saviano S, Ravalico G. Iris fluorescein angiography and iris indocyanine green videoangiography in pseudoexfoliation syndrome. Eur J Ophthalmol 1999;9:284–90.
4. Brancato R, Bandello F, Lattanzio R. Iris fluorescein angiography in clinical practice. Surv Ophthalmol 1997;42:41–70.
5. Ang M, Baskaran M, Werkmeister RM, Chua J, Schmidl D, Aranha Dos Santos V, et al. Anterior segment optical coherence tomography. Prog Retin Eye Res 2018;66:132–56.
6. Borrelli E, Sarraf D, Freund KB, Sadda SR. OCT angiography and evaluation of the choroid and choroidal vascular disorders. Prog Retin Eye Res 2018;67:30–55.
7. Ang M, Devarajan K, Tan AC, Ke M, Tan B, Teo K, et al. Anterior segment optical coherence tomography angiography for iris vasculature in pigmented eyes. Br J Ophthalmol. 2020: bjophthalmol-2020-316930.
8. Zett C, Stina DMR, Kato RT, Novais EA, Allemann N. Comparison of anterior segment optical coherence tomography angiography and fluorescein angiography for iris vasculature analysis. Graefe's Arch Clin Exp Ophthalmol 2018;256:683–91.

9. Ang M, Tan ACS, Cheung CMG, Keane PA, Dolz-Marco R, Sng CCA, et al. Optical coherence tomography angiography: a review of current and future clinical applications. Graefe's Arch Clin Exp Ophthalmol 2018 2562 2018;256:237–45.
10. Skalet AH, Li Y, Lu CD, Jia Y, Lee BK, Husvogt L, et al. Optical coherence tomography angiography characteristics of iris melanocytic tumors. Ophthalmology 2017;124:197–204.
11. Chien JL, Sioufi K, Ferenczy S, Say EAT, Shields CL. Optical coherence tomography angiography features of iris racemose hemangioma in 4 cases. JAMA Ophthalmol. 2017;135:1106–10.
12. Roberts PK, Goldstein DA, Fawzi AA. Anterior segment optical coherence tomography angiography for identification of iris vasculature and staging of iris neovascularization: a pilot study. Curr Eye Res 2017;42:1136–42.
13. Spaide RF, Fujimoto JG, Waheed NK. Image artifacts in Optical coherence tomography angiography. Retina 2015;35:2163–80.
14. Hogan MJ, Alvarado JA, Weddell JE. Histology of the human eye; an atlas and textbook. Philadelphia: Saunders; 1971.
15. Mozaed KT. Iris Anatomy. In: The Iris. 1st ed. Springer International Publishing; 2020. pp. 15–30.
16. Postolache L, Parsa CF. Brushfield spots and Wölfflin nodules unveiled in dark irides using near-infrared light. Sci Rep. 2018;8:1–6.
17. Moazed KT. Iris histology. The Iris. 1st ed. Springer International Publishing; 2020. p. 31–51.
18. Young B, Woodford P, O'Down G. The Eye. In: Elsevier (ed). Wheater's Funcional Histology, a Text and Colour Atlas. 6th ed.; 2013. pp. 404–15.
19. Brijesh K. Eye. In: Wolters Kluwer (ed). Histology Text & Atlas. 1st ed.; 2013. pp. 341–53.
20. Pichi F, Roberts P, Neri P. The broad spectrum of application of optical coherence tomography angiography to the anterior segment of the eye in inflammatory conditions: a review of the literature. J. Ophthalmic Inflamm. Infect. 2019;9:18.
21. Remington LA. Chapter 3, Uvea. Clin. Anat. Physiol Vis Syst 2012;1:40–60.
22. Song Y, Song YJ, Ko MK. A study of the vascular network of the iris using flat preparation. Korean J Ophthalmol 2009;23:296–300.
23. Wilcox LM, Keough EM, Connolly RJ, Hotte CE. The contribution of blood flow by the anterior ciliary arteries to the anterior segment in the primate eye. Exp Eye Res 1980;30:167–74.
24. Huang D, Swanson EA, Lin CP, Schuman JS, Stinson WG, Chang W, et al. Optical coherence tomography. Science 1991;254:1178–81.
25. Izatt JA, Hee MR, Swanson EA, Lin CP, Huang D, Schuman JS, et al. Micrometer-scale resolution imaging of the anterior eye in vivo with optical coherence tomography. Arch Ophthalmol (Chic, Ill 1960) 1994;112:1584–9.
26. Sheth V, Gottlob I, Mohammad S, McLean RJ, Maconachie GDE, Kumar A, et al. Diagnostic potential of iris cross-sectional imaging in albinism using optical coherence tomography. Ophthalmology. 2013;120:2082–90. Available at: https://doi.org/10.1016/j.ophtha.2013.03.018.
27. Invernizzi A, Giardini P, Cigada M, Viola F, Staurenghi G. Three-dimensional morphometric analysis of the iris by swept-source anterior segment optical coherence tomography in a caucasian population. Investig Ophthalmol Vis Sci 2015;56:4796–801.
28. Nakakura S, Nagata Y, Shimizu Y, Kawai A, Tabuchi H, Kiuchi Y. Determination of iris thickness development in children using swept-source anterior-segment optical coherence tomography. PLoS One. 2019;14:e0217656.
29. Invernizzi A, Cigada M, Savoldi L, Cavuto S, Fontana L, Cimino L. In vivo analysis of the iris thickness by spectral domain optical coherence tomography. Br J Ophthalmol 2014;98:1245–9.
30. Sidhartha E, Gupta P, Liao J, Tham Y-C, Cheung CY, He M, et al. Assessment of iris surface features and their relationship with iris thickness in Asian eyes. Ophthalmology. 2014;121:1007–12.
31. Schuster AK, Fischer JE, Vossmerbaeumer U. Curvature of iris profile in spectral domain optical coherence tomography and dependency to refraction, age and pupil size – the MIPH Eye&Health Study. Acta Ophthalmol. 2017;95:175–81.
32. Shi Y, Marion KM, Jenkins D, Sadda S, Le PV, Chopra V. Identification and characterization of imaging technique errors and artifacts using anterior-segment OCT for irido-corneal angle evaluations in glaucoma. Ophthalmol Glaucoma 2019;2:136–44.
33. Qiao Y, Tan C, Zhang M, Sun X, Chen J. Comparison of spectral domain and swept source optical coherence tomography for angle assessment of Chinese elderly subjects. BMC Ophthalmol. 2019;19:142.
34. Regatieri CV, Alwassia A, Zhang JY, Vora R, Duker JS. Use of optical coherence tomography in the diagnosis and management of uveitis. Int Ophthalmol Clin 2012;52:33–43.
35. Basarir B, Altan C, Pinarci EY, Celik U, Satana B, Demirok A. Analysis of iris structure and iridocorneal angle parameters with anterior segment optical coherence tomography in Fuchs' uveitis syndrome. Int Ophthalmol 2013;33:245–50.
36. Matsuki T, Hirose F, Ito SI, Hata M, Hirami Y, Kurimoto Y. Influence of anterior segment biometric parameters on the anterior chamber angle width in eyes with angle closure. J Glaucoma 2015;24:144–8.
37. Hirose F, Hata M, Ito SI, Matsuki T, Kurimoto Y. Light-dark changes in iris thickness and anterior chamber angle width in eyes with occludable angles. Graefe's Arch Clin Exp Ophthalmol 2013;251:2395–402.
38. Wang B, Sakata LM, Friedman DS, Chan YH, He M, Lavanya R, et al. Quantitative iris parameters and association with narrow angles. Ophthalmology. 2010;117:11–17. Available at: https://doi.org/10.1016/j.ophtha.2009.06.017.
39. Nongpiur ME, He M, Amerasinghe N, Friedman DS, Tay W-T, Baskaran M, et al. Lens vault, thickness, and position in Chinese subjects with angle closure. Ophthalmology. 2011;118:474–9.
40. Ramakrishnan R, Mitra A, Abdul Kader M, Das S. To study the efficacy of laser peripheral iridoplasty in the treatment of eyes with primary angle closure and plateau iris syndrome, unresponsive to laser peripheral iridotomy, using anterior-segment OCT as a tool. J Glaucoma 2016;25:440–6.
41. Shah A, Low S, Garway-Heath DF, Foster PJ, Barton K. Iris concavity, corneal biomechanics, and their correlations with ocular biometry in a cohort of 10- to 12-year-old UK school boys: Baseline data. Investig Ophthalmol Vis Sci 2014;55:3303–10.
42. Han SB, Liu YC, Noriega KM, Mehta JS. Applications of anterior segment optical coherence tomography in cornea and ocular surface diseases. J Ophthalmol. 2016;2016:4971572.
43. Krema H, Santiago RA, Gonzalez JE, Pavlin CJ. Spectral-domain optical coherence tomography versus ultrasound biomicroscopy for imaging of nonpigmented iris tumors. Am J Ophthalmol 2013;156:806–812.e1. https://doi.org/10.1016/j.ajo.2013.05.025.
44. Hau SC, Papastefanou V, Shah S, Sagoo MS, Restori M, Cohen V. Evaluation of iris and iridociliary body lesions with anterior segment optical coherence tomography versus ultrasound B-scan. Br J Ophthalmol 2015;99:81–6.
45. Pavlin CJ, Vásquez LM, Lee R, Simpson ER, Ahmed IIK. Anterior segment optical coherence tomography and ultrasound biomicroscopy in the imaging of anterior segment tumors. Am J Ophthalmol 2009;147:214–219.e2.
46. Bianciotto C, Shields CL, Guzman JM, Romanelli-Gobbi M, Mazzuca D, Green WR, et al. Assessment of anterior segment tumors with ultrasound biomicroscopy versus anterior segment optical coherence tomography in 200 cases. Ophthalmology. 2011;118:1297–302. https://doi.org/10.1016/j.ophtha.2010.11.011.
47. Chan TK, Rosenbaum AL, Rao R, Schwartz SD, Santiago P, Thayer D. Indocyanine green angiography of the anterior segment in patients undergoing strabismus surgery. Br J Ophthalmol 2001;85:214–8.
48. Gillies WE, Tangas C. Fluorescein angiography of the iris in anterior segment pigment dispersal syndrome. Br J Ophthalmol 1986;70:284–9.
49. Peiretti E, Iovino C. Chapter 9 - Indocyanine Green Angiography. In: Chhablani J (ed). Central Serous Chorioretinopathy. Academic Press; 2019. pp. 97–113. Available at: https://www.sciencedirect.com/science/article/pii/B9780128168004000097.
50. Choi W, Moult EM, Waheed NK, Adhi M, Lee B, Lu CD, et al. Ultrahigh-speed, swept-source optical coherence tomography angiography in nonexudative age-related macular degeneration with geographic atrophy. Ophthalmology. 2015;122:2532–44.
51. Devarajan K, Ong HS, Lwin NC, Chua J, Schmetterer L, Mehta JS, et al. Optical coherence tomography angiography imaging to monitor Anti-VEGF treatment of corneal vascularization in a rabbit model. Sci Rep. 2019;9:17576.
52. Ong HS, Tey KY, Ke M, Tan B, Chua J, Schmetterer L, et al. A pilot study investigating anterior segment optical coherence tomography angiography as a non-invasive tool in evaluating corneal vascularisation. Sci Rep. 2021;11:1212.
53. Ang M, Sim DA, Keane PA, Sng CCA, Egan CA, Tufail A, et al. Optical coherence tomography angiography for anterior segment vasculature imaging. Ophthalmology 2015;122:1740–7.
54. Velez FG, Davila JP, Diaz A, Corradetti G, Sarraf D, Pineles SL. Association of change in iris vessel density in optical coherence tomography angiography with anterior segment ischemia after strabismus surgery. JAMA Ophthalmol. 2018;136:1041–5.
55. Akagi T, Fujimoto M, Ikeda HO. Anterior segment optical coherence tomography angiography of iris neovascularization after intravitreal ranibizumab and panretinal photocoagulation. JAMA Ophthalmol. 2020;138:e190318.
56. Shiozaki D, Sakimoto S, Shiraki A, Wakabayashi T, Fukushima Y, Oie Y, et al. Observation of treated iris neovascularization by swept-source-based en-face anterior-segment optical coherence tomography angiography. Sci Rep. 2019;9:1–6.
57. Nagarkatti-Gude N, Li Y, Huang D, Wilson DJ, Skalet AH. Optical coherence tomography angiography of a pigmented Fuchs' adenoma (age-related hyperplasia of the nonpigmented ciliary body epithelium) masquerading as a ciliary body melanoma. Am J Ophthalmol Case Rep. 2018;9:72–4.
58. Williams BKJ, Di Nicola M, Ferenczy S, Shields JA, Shields CL. Iris microhemangiomatosis: clinical, fluorescein angiography, and optical coherence tomography angiography features in 14 consecutive patients. Am J Ophthalmol. 2018;196:18–25.

59. Pichi F, Sarraf D, Arepalli S, Lowder CY, Cunningham ETJ, Neri P, et al. The application of optical coherence tomography angiography in uveitis and inflammatory eye diseases. Prog Retin Eye Res 2017;59:178–201.

60. Siddiqui Y, Yin J. Anterior segment applications of optical coherence tomography angiography. Semin Ophthalmol 2019;34:264–9.

61. Lee WD, Devarajan K, Chua J, Schmetterer L, Mehta JS, Ang M, et al. Optical coherence tomography angiography for the anterior segment. Eye Vis (Lond, Engl). 2019;6:4.

62. Köse HC, Gündüz K, Hoşal MB. Iris cysts: Clinical features, imaging findings, and treatment results. Turkish J Ophthalmol. 2020;50:31–6.

63. Ayres M, Smallwood R, Brooks AM, Chan E, Fagan X. Anterior segment optical coherence tomography angiography. J Vis Commun Med 2019;42:153–7.

64. Kang AS, Welch RJ, Sioufi K, Say EAT, Shields JA, Shields CL. Optical coherence tomography angiography of iris microhemangiomatosis. Am J Ophthalmol case Rep. 2017;6:24–6.

65. Pichi F, Woodstock E, Hay S, Neri P. Optical coherence tomography angiography findings in systemic lupus erythematosus patients with no ocular disease. Int Ophthalmol 2020;40:2111–8.

66. Gao SS, Jia Y, Zhang M, Su JP, Liu G, Hwang TS, et al. Optical coherence tomography angiography. Invest Ophthalmol Vis Sci 2016;57:OCT27–36.

67. Hunter DG. Improving access-but not outcomes-with iris optical coherence tomography angiography. JAMA Ophthalmol. 2018;136:1045–6.

68. Spaide RF, Fujimoto JG, Waheed NK, Sadda SR, Staurenghi G. Optical coherence tomography angiography. Prog Retin Eye Res 2018;64:1–55.

69. Ang M, Cai Y, Tan ACS. Swept source optical coherence tomography angiography for contact lens-related corneal vascularization. J Ophthalmol 2016;2016:9685297.

70. Koprowski R, Foster KR. Machine learning and medicine: book review and commentary. Biomed Eng Online 2018;17:17.

71. Lanza M, Koprowski R, Bifani, Sconocchia M. Improving accuracy of corneal power measurement with partial coherence interferometry after corneal refractive surgery using a multivariate polynomial approach. Biomed Eng Online 2018;17:108.

72. Darcy AM, Louie AK, Roberts LW. Machine learning and the profession of medicine. JAMA 2016;315:551–2.

73. Lee A, Taylor P, Kalpathy-Cramer J, Tufail A. Machine learning has arrived! Ophthalmology 2017;124:1726–8.

74. Dembski M, Nowińska A, Ulfik-Dembska K, Wylęgała E. Swept source optical coherence tomography analysis of the selected eye's anterior segment parameters. J Clin Med 2021;10:1094.

75. Pujari A, Agarwal D, Sharma N. Clinical role of swept source optical coherence tomography in anterior segment diseases: a review. Semin. Ophthalmology. 2021;10:1–8.

76. Ang M, Devarajan K, Das S, Stanzel T, Tan A, Girard M, et al. Comparison of anterior segment optical coherence tomography angiography systems for corneal vascularisation. Br J Ophthalmol 2018;102:873–7.

77. Carnevali A, Mastropasqua R, Gatti V, Vaccaro S, Mancini A, D'aloisio R, et al. Optical coherence tomography angiography in intermediate and late age-related macular degeneration: Review of current technical aspects and applications. Appl Sci 2020;10:1–20.

78. Bacherini D, Mastropasqua R, Borrelli E, Capuano V, Iovino C, Dragotto F, et al. OCT-A in the management of vitreoretinal diseases and surgery. Asia-Pacific. J Ophthalmol 2021;10:12–9.

AUTHOR CONTRIBUTIONS

COMPETING INTERESTS

ADDITIONAL INFORMATION